Title
Coupled evolution of BrO_x-ClO_x-HO_x-NO_xchemistry during bromine-catalyzed ozone depletion events in the arctic boundary layer

Journal
Journal of Geophysical Research, 108(D4)

ISSN
0148-0227

Author
Evans, MJ

Publication Date
2003

DOI
10.1029/2002jd002732

Coupled evolution of BrO_x-ClO_x-HO_x-NO_x chemistry during bromine-catalyzed ozone depletion events in the arctic boundary layer

M. J. Evans,[1] D. J. Jacob,[1] E. Atlas,[2] C. A. Cantrell,[2] F. Eisele,[2,3] F. Flocke,[2] A. Fried,[2] R. L. Mauldin,[2] B. A. Ridley,[2] B. Wert,[2,4] R. Talbot,[8] D. Blake,[5] B. Heikes,[6] J. Snow[6,7], J. Walega,[2] A. J. Weinheimer,[2] and J. Dibb[8]

Received 8 July 2002; revised 8 October 2002; accepted 10 October 2002; published 28 February 2003.

[1] Extensive chemical characterization of ozone (O_3) depletion events in the Arctic boundary layer during the TOPSE aircraft mission in March–May 2000 enables analysis of the coupled chemical evolution of bromine (BrO_x), chlorine (ClO_x), hydrogen oxide (HO_x) and nitrogen oxide (NO_x) radicals during these events. We project the TOPSE observations onto an O_3 chemical coordinate to construct a chronology of radical chemistry during O_3 depletion events, and we compare this chronology to results from a photochemical model simulation. Comparison of observed trends in ethyne (oxidized by Br) and ethane (oxidized by Cl) indicates that ClO_x chemistry is only active during the early stage of O_3 depletion ($O_3 > 10$ ppbv). We attribute this result to the suppression of BrCl regeneration as O_3 decreases. Formaldehyde and peroxy radical concentrations decline by factors of 4 and 2 respectively during O_3 depletion and we explain both trends on the basis of the reaction of CH_2O with Br. Observed NO_x concentrations decline abruptly in the early stages of O_3 depletion and recover as O_3 drops below 10 ppbv. We attribute the initial decline to $BrNO_3$ hydrolysis in aerosol, and the subsequent recovery to suppression of $BrNO_3$ formation as O_3 drops. Under halogen-free conditions we find that HNO_4 heterogeneous chemistry could provide a major NO_x sink not included in standard models. Halogen radical chemistry in the model can produce under realistic conditions an oscillatory system with a period of 3 days, which we believe is the fastest oscillation ever reported for a chemical system in the atmosphere. *INDEX TERMS:* 0305 Atmospheric Composition and Structure: Aerosols and particles (0345, 4801); 0317 Atmospheric Composition and Structure: Chemical kinetic and photochemical properties; 0365 Atmospheric Composition and Structure: Troposphere—composition and chemistry; *KEYWORDS:* Polar, ozone, boundary layer, bromine, NO_x, HO_x

Citation: Evans, M. J., et al., Coupled evolution of BrO_x-ClO_x-HO_x-NO_x chemistry during bromine-catalyzed ozone depletion events in the arctic boundary layer, *J. Geophys. Res.*, *108*(D4), 8368, doi:10.1029/2002JD002732, 2003.

1. Introduction

[2] Events of near-total ozone (O_3) depletion in Arctic spring surface air have been observed since the 1980s [*Oltmans*, 1981; *Oltmans and Komhyr*, 1986] and are known to be due to fast catalytic loss driven by unusually high concentrations of bromine oxide radicals ($BrO_x \equiv Br + BrO$) [*Barrie et al.*, 1988; *Hausmann and Platt*, 1994]. These events are also associated with high concentrations of chlorine oxide radicals ($ClO_x \equiv Cl + ClO$) as demonstrated by observations of differential hydrocarbon depletion [*Yokouchi et al.*, 1994; *Jobson et al.*, 1994]. More recently, several studies have pointed out the importance of polar snow as a source of nitrogen oxide radicals ($NO_x \equiv NO + NO_2$) and of precursors of hydrogen oxide radicals ($HO_x \equiv$ OH + peroxy radicals) during spring [*Sumner and Shepson*, 1999; *Honrath et al.*, 2000; *Jones et al.*, 2001]. Extensive chemical observations during the Tropospheric Ozone Production around the Spring Equinox (TOPSE) aircraft campaign [*Atlas et al.*, 2003] offer the first opportunity to analyze the coupled evolution of BrO_x-ClO_x-NO_x-HO_x radical chemistry during O_3 depletion events in the Arctic spring. We present such an analysis here and use photochemical model calculations to place the TOPSE observations in the context of current understanding.

[3] The bromine chemistry leading to O_3 depletion is relatively well understood [*Barrie et al.*, 1988; *Fan and*

[1]Division of Engineering and Applied Science, Harvard University, Cambridge, Massachusetts, USA.
[2]Atmospheric Chemistry Division, National Center for Atmospheric Research, Boulder, Colorado, USA.
[3]Also at Georgia Institute of Technology, Atlanta, Georgia, USA.
[4]Chemistry Department, University of Colorado, Boulder, Colorado, USA.
[5]Chemistry Department, University of California, Irvine, Irvine, California, USA.
[6]School of Oceanography, University of Rhode Island, Narragansett, Rhode Island, USA.
[7]Now at University of Washington Bothell, Bothell, Washington, USA.
[8]Climate Change Research Center, University of New Hampshire, Durham, New Hampshire, USA.

0148-0227/03/2002JD002732

Jacob, 1992; *Hausmann and Platt*, 1994; *Michalowski et al.*, 2000]. It involves the catalytic O_3 destruction by BrO_x radicals and it requires the recycling of BrO_x from its non-radical reservoirs. The main catalytic mechanism for O_3 depletion is

$$\text{(R1)} \qquad 2 \times (Br + O_3 \rightarrow BrO + O_2)$$

$$\text{(R2)} \qquad BrO + BrO \rightarrow Br_2 + O_2$$

$$\text{(R3)} \qquad \text{Net } \frac{Br_2 + h\nu \rightarrow 2Br}{2O_3 \rightarrow 3O_2}$$

[4] The efficiency of this cycle is limited by conversion of BrO_x to the non-radical reservoir HBr, which is long-lived with respect to both photolysis and reaction with OH. Production of HBr is mostly by the reaction between Br and CH_2O, although reactions with other carbonyls can also be significant [*Shepson et al.*, 1996].

$$\text{(R4)} \qquad Br + CH_2O \rightarrow HBr + CO + HO_2$$

[5] The HBr is readily soluble and dissolves in aerosols to release bromide (Br^-) in solution. Similarly, the other non-radical bromine reservoirs $BrNO_3$ (produced from NO_2 + BrO) and HOBr (produced from HO_2 + BrO) are taken up by aerosol, where $BrNO_3$ hydrolyzes to HOBr [*Hanson et al.*, 1996]. In acidic aerosols, as are observed in the Arctic spring [*Sirois and Barrie*, 1999], HOBr reacts with Br^- to produce Br_2, which escapes into the gas phase and is photolysed:

$$\text{(R5)} \qquad Br^- + HOBr + H^+ \rightarrow Br_2 + H_2O$$

$$\text{(R3)} \qquad Br_2 + h\nu \rightarrow 2Br$$

[6] In this manner the radical bromine is regenerated, sustaining the O_3 loss cycle (R1–R3). Although there is now substantial evidence from field and laboratory studies to support the above mechanism, model calculations of the O_3 loss rate in relation to the BrO_x radical supply have never been evaluated with observations. We will present such an evaluation here and examine the chemical coupling of BrO_x with other radical families.

[7] A complicating factor for the NO_x and HO_x radical budgets in the Arctic boundary layer is the emission of NO_x and CH_2O from the snow surface. These emissions appear to be driven by sunlight [*Sumner and Shepson*, 1999; *Ridley et al.*, 2000; *Honrath et al.*, 2000; *Jones et al.*, 2001] although physical adsorption and desorption may also take place [*Hutterli et al.*, 1999, 2001]. Surface measurements at Alert in the Canadian Arctic show a pronounced diurnal cycle of NO_x concentrations [*Ridley et al.*, 2000] with a noon maximum, suggesting a shorter lifetime for NO_x (less than 4 hours) than would be expected from atmospheric loss by oxidation in standard models. We include the snow emissions of NO_x and CH_2O in our analysis and propose that heterogeneous oxidation of HNO_4 in aerosols provides a major sink of NO_x in the Arctic boundary layer.

[8] Section 2 describes the O_3 depletion events observed during TOPSE with focus on the evolution of radical chemistry. We apply a photochemical model (section 3) to simulate the chemical development of these events and interpret the TOPSE observations (section 4). An intriguing chemical oscillation taking place in the model under certain conditions is presented in section 5. Conclusions are in section 6.

2. Ozone Depletion Events Observed During TOPSE

[9] The TOPSE aircraft program took place between February and May 2000 [*Atlas et al.*, 2003]. Its goal was to investigate the origin of the springtime O_3 maximum observed at northern extra-tropical latitudes [*Monks*, 2000]. The NSF C-130 aircraft flew between Boulder (Colorado), Churchill (Manitoba), and Thule (Greenland), with some flights north to 85°N over the Arctic Ocean. A total of 37 flights were carried out (see Figure 1). The aircraft carried a wide range of chemical instrumentation including measurements of O_3, NO_x and total reactive nitrogen oxides (NO_y) [*Ridley et al.*, 2003], speciated hydrocarbons [*Blake et al.*, 2003], OH [*Mauldin et al.*, 2003], total peroxy radicals (RO_2) (C. A. Cantrell et al., Peroxy radical observations using CIMS during TOPSE, manuscript submitted to J. Geophys. Res., 2002), H_2O_2 and CH_3OOH [*Snow et al.*, 2003], CH_2O [*Fried et al.*, 2003], peroxyacetyl nitrate (PAN) and soluble bromide [*Scheuer et al.*, 2003]. Photolysis frequencies [*Shetter and Mueller*, 1999] and aerosol size distributions were also measured. Individual cases of O_3 depletion events observed during TOPSE are discussed by *Ridley et al.* [2003].

[10] Figure 2 shows the cumulative probability distribution of O_3 concentrations observed in the Arctic boundary layer (below 500 m altitude and north of 50°N) during spring (March 23 to May 22) and around local noon (1100 to 1300). Most TOPSE data were collected around midday; introducing the 1100 to 1300 restriction filters out 50% of the data and makes little change to the distribution. The O_3 concentrations range from 0.2 to 50 ppbv; 50% of the measurements are below 23 ppbv. The accuracy of the O_3 measurements was 0.06 ppbv at 1 ppbv of O_3 [*Ridley et al.*, 2003]. For further analysis we partitioned the data into four O_3 bins (0 to 1 ppbv, 1 to 10 ppbv, 10 to 30 ppbv and above 30 ppbv). Table 1 gives the means and standard deviations of the ensemble of TOPSE observations in these four bins. Selection of data below 100 m rather than 500 m leads to an increased probability of low O_3 concentrations but little change to the concentration of species within each O_3 bin. We will assume in what follows that differences in composition between the four categories of air masses in Table 1 reflect different degrees of processing by halogen radical chemistry. In support of this assumption, we see in Table 1 that CO (unaffected by halogen chemistry) is uniform across all four categories.

[11] Soluble bromide concentrations observed during TOPSE are highest in the O_3 depleted air masses. Ethyne and ethane show differing trends as O_3 decreases. Whereas the ethyne concentration drops continuously with O_3, the ethane concentration changes little below 10 ppbv of O_3. We propose in section 4.2 that this reflects different temporal evolutions of bromine and chlorine radicals during O_3 depletion events. Concentrations of HO_x radicals and reservoir species (OH, RO_2, CH_2O, H_2O_2 and CH_3OOH) all

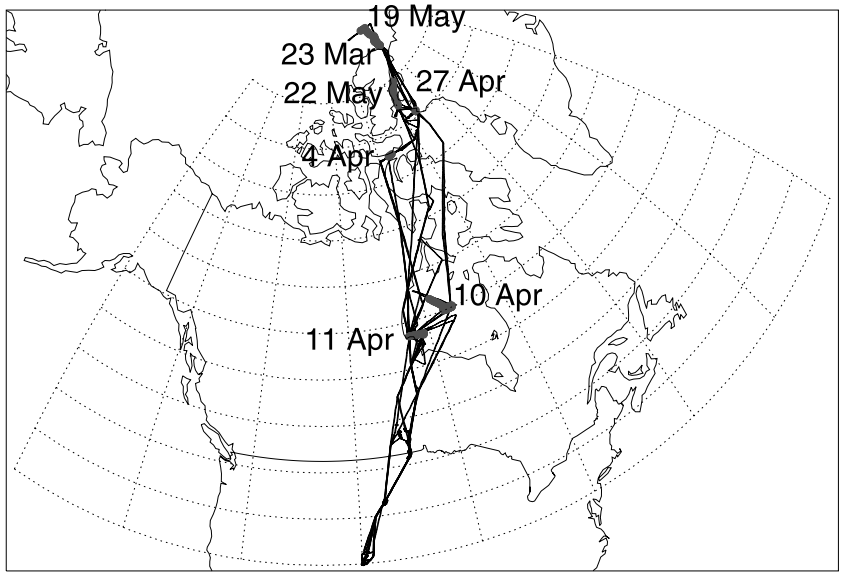

Figure 1. Flight tracks during TOPSE (February–May 2000). Symbols show location of boundary layer tracks (below 500 m altitude) with O_3 concentrations less than 15 ppbv. The dates during which these air masses were encountered are given.

decrease with decreasing O_3 concentration. A previous study of CH_2O evolution during O_3 depletion events observed at Alert [*Rudolph et al.*, 1999] showed a gradual increase in CH_2O concentrations from 40 to 15 ppbv of O_3 followed by a decline similar to that observed during TOPSE. The budgets of these species are discussed in section 4.3

[12] Concentrations of NO_x observed in TOPSE decrease as O_3 drops below 30 ppbv but then recover as O_3 drops below 10 ppbv, so that concentration under conditions of strong O_3 depletion ($O_3 < 1$ ppbv) are similar to those with little or no depletion ($O_3 > 30$ ppbv). The initial reduction in NO_x at the onset of O_3 depletion events has been seen before [*Beine et al.*, 1997]. Concentrations of NO_y appear to increase slightly as the O_3 concentration decreases and PAN concentrations shows a more substantial increase. These intriguing trends in the NO_y species are examined further in section 4.4.

3. Photochemical Model

[13] We apply a 0-D (box) photochemical model of the Arctic boundary layer to interpret the relationships described above and examine the coupled evolution of BrO_x-ClO_x-HO_x-NO_x radical chemistry during O_3 deple-

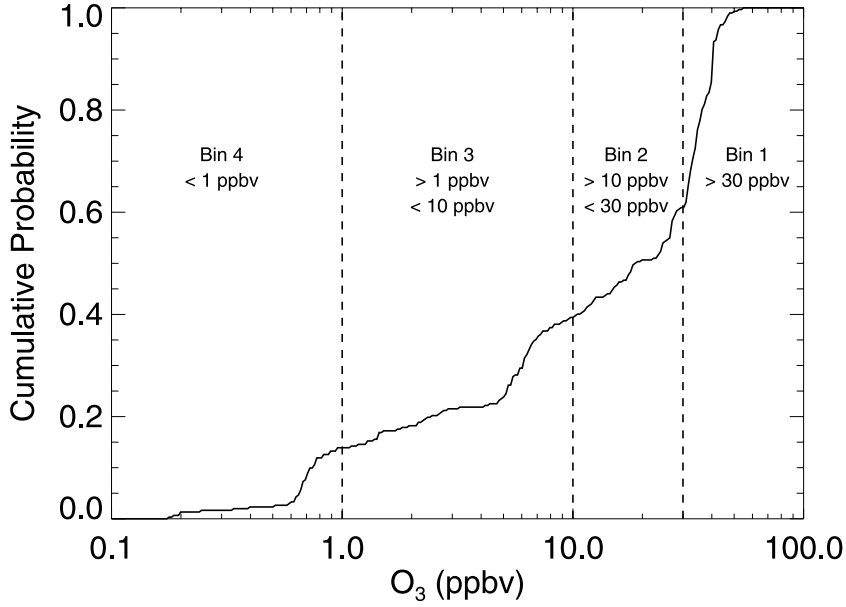

Figure 2. Cumulative probability distribution of midday (1100 to 1300 local time) O_3 concentrations measured north of 50°N and below 500 m altitude between March 23 and May 22 during TOPSE. 252 1-minute measurements are included in the distribution. The dashed lines define the O_3 bins used for analysis.

Table 1. Arctic Boundary Layer Observations During TOPSE[a]

	Bin 1	Bin 2	Bin 3	Bin 4	Background
Ozone Range (ppbv)	>30	10 − 30	1 − 10	<1	Note b
Day of year	107 ± 26	108 ± 23	107 ± 13	105 ± 9	106.7
Latitude (°N)	72 ± 9	77 ± 8	74 ± 10	67 ± 11	73
Longitude (°E)	−77 ± 12	−70 ± 11	−75 ± 10	−78 ± 12	−75
Altitude (m)	144 ± 140	96 ± 107	97 ± 104	52 ± 57	100
O_3 column (DU)	370 ± 42	371 ± 55	428 ± 67	470 ± 59	398
Aerosol area (10^{-7} cm^2/cm^3)[c]	4.7 ± 2.5	3.8 ± 2.0	5.3 ± 1.0	4.7 ± 1.2	4.9
Aerosol volume (10^{-12} cm^3/cm^3)[c]	4.2 ± 3.0	3.7 ± 3.4	4.5 ± 0.95	4.1 ± 1.3	4.4
H_2O (g/kg)	1.4 ± 0.8	0.88 ± 0.54	0.76 ± 0.35	0.71 ± 0.35	1.06
O_3 (ppbv)	38 ± 5	22 ± 6.1	5.0 ± 2.3	0.65 ± 0.21	48
CO (ppbv)	153 ± 10	151 ± 10	156 ± 4	157 ± 3	153
CH_4 (ppmv)	1.84 ± 0.01	1.85 ± 0.01	1.85 ± 0.01	1.85 ± 0.01	1.84
Soluble Bromide (pptv)[d]	7.8 ± 5	12.9 ± 9.4	23.0 ± 8.5	23.6 ± 2.8	Note e
Ethane (pptv)	1578. ± 302	1401 ± 341	1256 ± 162	1134 ± 152	1660
Ethyne (pptv)	347 ± 143	284 ± 125	119 ± 60	42 ± 28	389
Propane (pptv)	423 ± 250	352 ± 198	234 ± 85	179 ± 62	484
n-Butane (pptv)	109 ± 90	87 ± 61	40 ± 23	26 ± 13	136
i-Butane (pptv)	64 ± 52	63 ± 36	34 ± 18	25 ± 12	73
n-Pentane (pptv)	32 ± 15	19 ± 9.3	7.2 ± 3.6	4.3 ± 1.3	48
i-Pentane (pptv)	41 ± 20	31 ± 12	11 ± 6.3	6.5 ± 2.7	62
Hexane (pptv)	10 ± 4	6.8 ± 1.6	3.8 ± 0.5	<3[f]	15
OH ($\times$ 10^5 cm^{-3})	11. ± 9	5.0 ± 3.6	2.7 ± 2.1	1.7 ± 1.4	N/A
RO_2 ($\times$ 10^8 cm^{-3})[g]	2.2 ± 1.2	1.9 ± 1.2	1.3 ± 0.6	1.6 ± 0.4	N/A
CH_2O (pptv)	143 ± 104	137 ± 93	94 ± 89	35 ± 110	143
H_2O_2 (pptv)	264 ± 128	183 ± 113	92 ± 41	92 ± 74	254
CH_3OOH (pptv)	240 ± 123	230 ± 99	151 ± 43	131 ± 40	206
NO_x (pptv)	13 ± 8	4.6 ± 7.3	5.2 ± 4.7	15.0 ± 4.8	16
NO (pptv)	5.0 ± 5.0	1.1 ± 4.6	2.9 ± 3.2	11.7 ± 4.2	7.0
NO_2 (pptv)	7.5 ± 4	3.4 ± 3.7	2.4 ± 2.4	3.2 ± 2.1	9.9
NO_y (pptv)[h]	225 ± 39	200 ± 38	258 ± 16	253 ± 13	N/A
PAN (pptv)	152 ± 16	163 ± 39	212 ± 25	207 ± 10	161

[a]Means and standard deviations of aircraft observations made north of 50°N below 500 m altitude, from March 23 to May 22, 2000 and around local noon (1100–1300). The data are partioned by O_3 concentration range (see text) to determine the chemical characteristics of O_3 depletion events.

[b]Mean concentrations of species in air masses with $O_3 > 45$ ppbv and no detected soluble bromide. These concentrations are used as initial condition for the model simulation (Section 3). Initial condition for species not measured during TOPSE are given in section 3.

[c]Integrated over the 0.1–3 μm aerosol size distribution.

[d]Soluble bromide in gas (HBr) and aerosol phase (Br^-).

[e]Model simulations are conducted with initial bromide concentrations in the range 0–43 pptv [*Sirois and Barrie*, 1999].

[f]Below level of detection (~3 pptv).

[g]RO_2 is the sum of all peroxy radicals (HO_2 + organic peroxy radicals).

[h]NO_y is the sum of all gas phase nitrogen oxide species (NO, NO_2, NO_3, 2 × N_2O_5, HNO_2, HNO_3, HNO_4, organic nitrates).

tion events. We do not consider IO_x chemistry as there is little evidence to suggest that it plays an important role in the evolution of these O_3 depletion events [*Sander et al.*, 1997; *Martinez et al.*, 1999]. The model does not consider the deposition or emission of halogens to or from the snow surface and thus assumes that the bromine cycling within the aerosol is the dominant bromine activation mechanism (in general agreement with *Michalowski et al.* [2000]), and that the sole source and reservoir of bromine is the aerosol.

[14] The chemistry scheme used in the model has been described before [e.g., *Jaeglé et al.*, 2000] and has been extended here to include halogen and aerosol chemistry following *Michalowski et al.* [2000]. It includes a detailed description of the oxidation of C_1-C_6 hydrocarbons updated with recent developments [*Sander et al.*, 2000]. The rate constants for the reactions of Br with aldehydes [*Ramacher et al.*, 2000] and ethyne [*Ramacher et al.*, 2001] have been updated. Reactions of BrO with CH_2O and HBr are not included, based on evidence that they are negligibly slow; even at the upper limits reported by *Orlando et al.* [2000] we find that they have little effect on the evolution of O_3 depletion. Photolysis frequencies are calculated with a clear-sky radiative transfer model and are scaled to the mean midday photolysis frequencies of NO_2 ($J(NO_2)$) and $O_3 \rightarrow O(^1D)$ ($J(O^1D)$). The $J(O^1D)$ scaling factor is applied to wavelengths less than 330 nm and the $J(NO_2)$ scaling factor to higher wavelengths. Aerosol processes in the chemical mechanism are listed in Tables 2a and 2b and include halogen radical as well as HNO_4 chemistry.

[15] The model is initialized on April 15 at 73°N, at local noon at 100 m altitude, with TOPSE measurements representative of background Arctic conditions unaffected by halogen chemistry (Table 1: Background). The composition of the boundary layer aerosol is derived from previous studies. We assume that the bulk of the aerosol is sulfuric acid [*Barrie and Hoff*, 1984]. Aerosol concentrations per volume of air of Cl^- (100 ng m^{-3}, equivalent to 1.7×10^9 cm^{-3}) and I^- (0.3 ng m^{-3}, equivalent to 1.4×10^6 cm^{-3}) are taken from *Sirois and Barrie* [1999]; we assume that 50% of total iodine reported in *Sirois and Barrie* [1999] is iodide [*Baker et al.*, 2001]. An aerosol pH of 0.5 is assumed from *Li* [1994]. An initial aerosol HNO_2 concentration of 8×10^7 cm^{-3} (again referenced to volume of air) is also taken from Li [1994]. Aerosol concentrations of H^+, I^-, and

Table 2a. Aerosol Chemistry: Aqueous-Phase Reactions

Reaction	Rate Constant ($(M^{-1})^n$ s^{-1})	Reference
$HNO_4 + HSO_3^- \rightarrow SO_4^{2-} + NO_3^- + 2\ H^+$	$1.1 \times 10^7\ [H^+] + 3.3 \times 10^5$	*Amel et al.* [1996]
$HNO_4 + HNO_2 \rightarrow 2\ NO_3^- + 2\ H^+$	12	*Løgager and Sehested* [1993]
$HNO_4 + Cl^- \rightarrow HOCl + NO_3^-$	0.014	*Régimbal and Mozurkewich* [1997]
$HNO_4 + Br^- \rightarrow HOBr + NO_3^-$	0.54	*Régimbal and Mozurkewich* [1997]
$HNO_4 + I^- \rightarrow HOI + NO_3^-$	890	*Régimbal and Mozurkewich* [1997]
$Br^- + O_3 + H^+ \rightarrow HOBr + O_2$	11.7	*Haag and Hoigné* [1983]
$HOBr + Cl^- + H^+ \rightarrow BrCl + H_2O$	5.6×10^9	*Wang et al.* [1994]
$HOBr + Br^- + H^+ \rightarrow Br_2 + H_2O$	1.6×10^{10}	*Beckwith et al.* [1996]
$HOCl + Cl^- + H^+ \rightarrow Cl_2 + H_2O$	2.2×10^4	*Wang and Margerum* [1994]
$HOCl + Br^- + H^+ \rightarrow BrCl + H_2O$	1.3×10^6	*Kumar and Margerum* [1987]
$BrCl + H_2O \rightarrow HOBr + Cl^- + H^+$	1.0×10^5	*Wang et al.* [1994]
$Br_2 + H_2O \rightarrow HOBr + Br^- + H^+$	9.7×10^1	*Beckwith et al.* [1996]
$Cl_2 + H_2O \rightarrow HOCl + Br^- + H^+$	2.2×10^1	*Wang and Margerum* [1994]
$BrCl + Br^- \rightarrow Br_2Cl^-$	5×10^9	Note a
$Br_2 + Cl^- \rightarrow Br_2Cl^-$	5×10^9	Note a
$BrCl + Cl^- \rightarrow BrCl_2^-$	5×10^9	Note a
$Br_2Cl^- \rightarrow Br_2 + Cl^-$	3.9×10^9	Note b
$Br_2Cl^- \rightarrow BrCl + Br^-$	2.8×10^8	Note b
$BrCl_2^- \rightarrow Cl_2 + Cl^-$	6.9×10^2	Note b
$HBr \rightarrow Br^- + H^+$	0.3[c]	*Schweitzer et al.* [2000]
$HCl \rightarrow Cl^- + H^+$	0.3[c]	*Schweitzer et al.* [2000]
$BrNO_3 + H_2O \rightarrow HOBr + NO_3^- + H^+$	0.3[c]	*Hanson et al.* [1996]
$ClNO_3 + H_2O \rightarrow HOCl + NO_3^- + H^+$	0.002[c]	*Robinson et al.* [1997]
$N_2O_5 + H_2O \rightarrow 2\ NO_3^- + 2\ H^+$	0.1[c]	*Jacob* [2000]

[a]Assumed [*Michalowski et al.*, 2000].
[b]Derived from the equilibrium constant [*Wang et al.*, 1994] and the assumed forward rate constant (see footnote a).
[c]Reaction probabilities (γ), dimensionless.

HNO_2 are kept constant in the simulation but the Cl^- concentration is allow to evolve. I^- and HNO_2 are included in the model as aerosol-phase sinks of HNO_4 (see later) and play no further chemical role. Concentrations of CH_3CHO (18 pptv) and $(CH_3)_2CO$ (300 pptv) are assumed from chemical steady state with the background hydrocarbon concentrations given in Table 1.

[16] The boundary layer in our model is taken to be dynamically isolated from the free troposphere (zero flux boundary conditions at boundary layer top). This is a reasonable assumption for O_3 depletion events in general [*Wessel et al.*, 1998] and TOPSE in particular [*Ridley et al.*, 2003]. The surface is assumed to be snow and to provide a source or sink of nitrogen oxides, H_2O_2, and CH_2O. The surface flux boundary conditions for these and other non-radical secondary species are chosen to reproduce observed concentrations in background air (Background: Table 1) in a steady state calculation; for that purpose the boundary layer represented by the model is assumed to be 200m deep. We thus specify small deposition velocities for PAN, PPN and H_2O_2 (0.004 cm s^{-1}, 0.008 cm s^{-1}, and 0.09 cm s^{-1} respectively). Emission of NO_x and CH_2O from the snow surface is necessary to reproduce the observed concentrations with the model. We assume that these emissions vary diurnally following the photolysis of NO_2. The resulting 24-hour average emissions of CH_2O and NO_x are 1.2×10^9 cm^{-2} s^{-1} and 3.6×10^8 cm^2 s^{-1} respectively. Our implied CH_2O emission is a factor of 4 less than that found by *Sumner and Shepson* [1999]. This is mainly due to differing assumptions for the boundary layer height in the calculation (600m in *Sumner and Shepson* [1999] and 200 m in this work). Our implied NO_x emission is roughly 4 times higher than that observed by *Jones et al.* [2001] in Antarctica; such a difference could be rationalized as reflecting higher nitrate concentrations in the Arctic snow compared to the Antarctic [*Wolff et al.*, 1995]. It is in reasonable agreement (40% higher) with measurements made at Summit, Greenland during the summer of 2000 [*Honrath et al.*, 2002].

Table 2b. Aerosol Chemistry: Henry's Law Equilibria (H) and Mass Accomodation Coefficients (α)

Species	H (M/atm) 250K	α	References
$HOBr(g) \leftrightarrow HOBr$ (aer)	3.0×10^4	0.3	H: *Waschewsky and Abbatt* [1999] α: *Allanic et al.* [1997]
$HOCl(g) \leftrightarrow HOCl$(aer)	1.8×104	0.3	H: *Huthwelker et al.* [1995] α: *Abbat and Molina* [1992]
Br_2 (g) $\leftrightarrow$ Br_2 (aer)	1.0×10^1	0.01	H: *Kelley and Tartar* [1956] α: (estimated) *Sander and Crutzen* [1996]
Cl_2 (g) $\leftrightarrow$ Cl_2 (aer)	3.7×10^1	0.01	H: *Wilhelm et al.* [1977] α: (estimated) *Sander and Crutzen* [1996]
BrCl (g) $\leftrightarrow$ BrCl (aer)	5.6×10^1	0.01	H: *Bartlett and Mergerum* [1999] α: (estimated) *Sander and Crutzen* [1996]
O_3 (g) $\leftrightarrow$ O_3 (aer)	3.5×10^1	0.002	H: *Kosak-Channing and Helz* [1983] α: *Magi et al.* [1997]
HNO_4 (g) $\leftrightarrow$ HNO_4 (aer)	1.2×10^4	0.05	H: *Régimbal and Mozurkewich* [1997] α: *Li et al.* [1996]

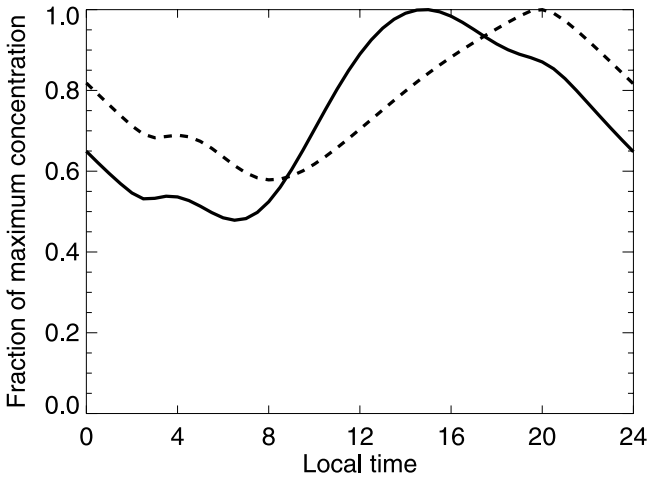

Figure 3. Normalized diurnal profile of NO_x ($NO + NO_2$) concentration simulated in the model with heterogeneous HNO_4 chemistry (solid line) and without (dashed line). Concentrations are normalized to the maximum concentration calculated over the diurnal cycle. Results are from a steady state Arctic boundary layer simulation for background conditions (Table 1) and no BrO_x-ClO_x chemistry.

[17] We find that the uptake of HNO_4 by aerosols and its subsequent reaction in the aerosol phase (mostly with HNO_2 and I^-) provides a significant NO_x sink in the Arctic boundary layer outside of O_3 depletion episodes. It accounts in the model for 40% of the NO_x loss on a 24-hour average basis and 50% at noon. This heterogeneous HNO_4 chemistry increases the amplitude of the diurnal cycle of NO_x concentrations and shifts the diurnal maximum to mid afternoon, as compared to a sensitivity simulation with no HNO_4 uptake by aerosols (Figure 3). The rate of the aerosol HNO_4 sink is limited by the rate of reaction in the aerosol phase, which in turn depends on the assumed concentration of reactants [*Sirois and Barrie*, 1999; *Li*, 1994]. The amplification of the diurnal cycle of NO_x concentrations due to HNO_4 chemistry in our model is consistent with the Alert observations of *Ridley et al.* [2000], but the timing of the model maximum (1400 local time) is still later than observed (1200) suggesting that the lifetime of NO_x in the measurements of *Ridley et al.* [2000] may be even shorter than that calculated here.

[18] Previous studies [*Warneck*, 1999; *Leriche et al.*, 2000; *Dentener et al.*, 2002] have shown the importance of HNO_4 in the oxidation of S(IV) in clouds. Our understanding of the role of HNO_4 in the atmospheric chemistry system is limited by both a lack of field observations and uncertainties in its chemistry (for example at 250K its thermal dissociation constant is uncertain by a factor of 10 [*DeMore et al.*, 1997]).

4. Radical Chemistry During Ozone Depletion Events

4.1. Temporal Evolution and O_3 Chemical Coordinate

[19] Starting from the steady state background conditions described in the previous section and summarized in Table 1, the model atmosphere was perturbed instantaneously with varying levels of bromide (Br^-) from 0.2 to 43 pptv (range observed by *Sirois and Barrie* [1999]) and then allowed to evolve chemically for 10 days. The initial activation of the halogen radicals is through the reactions of Br^- and O_3 [*Haag and Hoigné*, 1983] and HNO_4 [*Régimbal and Mozurkewich*, 1997] to release HOBr. After this initial activation, the recycling of bromine radicals from non-radical reservoirs is controlled by $Cl^- + HOBr + H^+ \rightarrow BrCl + H_2O$ [*Wang et al.*, 1994] and $Br^- + HOBr + H^+ \rightarrow Br_2 + H_2O$ [*Beckwith et al.*, 1996], with the recycling of Br^- being dominated by the latter.

[20] Figure 4 shows the temporal evolution of O_3, ethyne, NO_x ($NO + NO_2$) and BrO concentrations over 10 days for 3 of the cases (0, 13 and 43 pptv initial bromide). Without any bromine the model is at steady state for the radicals and their reservoirs; ethyne concentration decreases very slowly due to reaction with OH. With 13 pptv of initial bromide the O_3 concentration drops slowly from 45 to 30 ppbv over the 10 days of the simulation. This is accompanied by a slow linear loss of ethyne. The NO_x concentration drops precipitously due to $BrNO_3$ hydrolysis. The formation of $BrNO_3$ is favored toward dawn and dusk when Br/BrO and NO/NO_2 ratios are low, leading to a large diurnal cycle in the NO_x concentration. The small increases in NO_x concentrations simulated during night are due to the slow thermal decay of PAN and HNO_4. The daytime BrO concentrations remain steady at 9 pptv. If the concentration of initial bromide is increased to 43 pptv, the impact is much greater. O_3 concentrations drop down to a steady state of 1–2 ppbv after 6 days. As the O_3 concentration drops below 3 ppbv the bromine radical chemistry essentially shuts down, as seen in the disappearance of BrO and the leveling off of ethyne. This suppression of bromine radical chemistry is due to a change in the balance between gas-phase and aerosol-phase bromine. As the O_3 concentration drops, the NO/NO_2 and Br/BrO concentration ratios increase. Eventually, HOBr production by $BrO + HO_2$ is suppressed, preventing the recycling of bromine radicals by R5. The suppression of bromine radical chemistry and the increase in the NO/NO_2 ratio suppress in turn the formation of $BrNO_3$. The longer NO_x lifetime, together with the surface source, allows the NO_x concentration to recover.

[21] Simulations of the temporal evolution of O_3 and halogen radical concentrations in the Arctic boundary layer during O_3 depletion events have been reported in previous model studies [*Sander et al.*, 1997; *Michalowski et al.*, 2000]. Important new aspects here include the depletion and recovery of NO_x driven by $BrNO_3$ hydrolysis, and the coupling of Br and Cl chemistry which affects the evolution of ethyne and alkanes differently, as discussed below. As in previous modeling studies [e.g., *Sander et al.*, 1997], we find that the BrO self reaction is the dominant mechanism for halogen-catalyzed O_3 loss (~70%), with $BrO + HO_2$ playing a subsidiary role (~25%). Other mechanisms ($BrO + CH_3O_2$, $BrNO_3$ + aerosol, and ClO + BrO) play minor roles (~1%).

[22] It is difficult to compare this temporal evolution in the model directly with the TOPSE observations, which were not collected in a Lagrangian framework, and this has been a general problem in the evaluation of models of Arctic O_3 depletion. In order to enable such a comparison, we use the O_3 concentration as a proxy for chemical history and make the comparison along this chemical coordinate

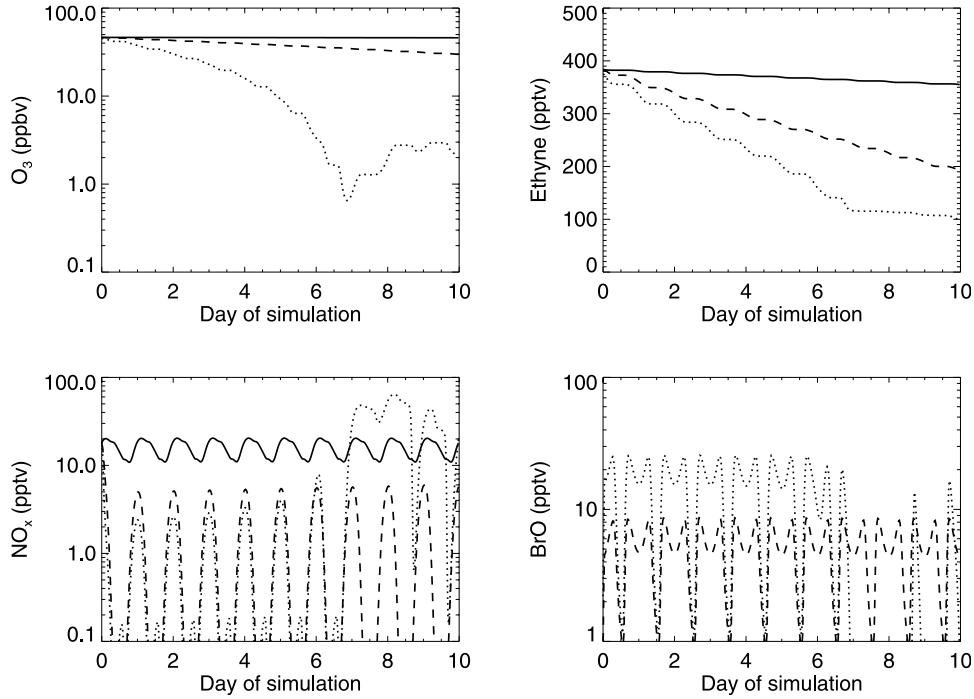

Figure 4. Simulated evolution of O_3, ethyne, NO_x (NO + NO_2) and BrO concentrations over 10 days with 3 different initial aerosol phase bromide concentrations (zero (continuous line), 13 pptv (dashed line) and 43 pptv (dotted line)). Initialization is at local noon.

(Figure 5) for different initial bromide concentrations. The observed relationships apparent in Figure 5 between the different species and O_3 concentration were previously discussed in section 2. Many of these relationships are reproduced by the model and the mechanisms leading to them can therefore be elucidated.

4.2. Halogen Radicals and Hydrocarbons

[23] The TOPSE observations show a decrease of the hydrocarbon concentrations along with O_3 (Table 1) reflecting the presence of both Br and Cl radicals. The model reproduces the observed trends, as shown in Figure 5 for ethyne and ethane. The differing behavior of ethyne and ethane reflects different temporal evolution of Br atoms (ethyne oxidant) and Cl atoms (ethane oxidant) as the O_3 concentrations drop (see for example *Ramacher et al.* [1999]). Bromine chemistry continues to operate at low O_3 concentrations (the ethyne concentration declines at all O_3 concentrations) whereas chlorine chemistry is quenched below 10 ppbv of O_3 (ethane is not depleted further).

[24] Figure 6 describes the simulated evolution of the concentrations of halogen species as the O_3 concentration drops. Chlorine radical concentrations drop to near zero below 5 ppbv of O_3. A number of processes contribute to this decline. The only significant source of chlorine radicals in the model is the reaction of aerosol Cl^- with HOBr to produce BrCl which volatilizes and photolyses. The Cl^- concentration remains essentially constant during the simulation (Figure 6) so that the production of active chlorine is limited by the availability of HOBr. As the O_3 concentration drops, the production of HOBr decreases (as discussed previously), reducing the production of BrCl. The production of Br^- increases, so that the reaction of Br^- and HOBr competes with the reaction of Cl^-, further reducing the conversion of Cl^- into BrCl. The increase in Br^- also increases the rate of the reaction between Br^- and BrCl to produce Br_2Cl^-, which predominantly decomposes to Br_2 and Cl^-.

[25] In contrast to Cl, the concentration of Br atoms increases initially as O_3 declines, and remains relatively high even as O_3 drops down to 1 ppbv. The reduction in the HOBr concentration as the O_3 drops is to some extent compensated for by an increase in the Br^- concentration, so that overall the rate of volatilization of Br_2 from the aerosol is maintained. Increasing Br/BrO ratio as the O_3 concentration declines further contributes to maintaining high Br atom concentrations.

4.3. Hydrogen Oxide Radicals

[26] We find that the RO_2 concentration drops by a factor of 2, both in the model and in the observations, as O_3 concentrations decrease from background values down to 1 ppbv (Figure 5). Measured OH declines by a factor of 5 while simulated OH declines by only a factor of 2. Problems with the OH instrumentation [*Mauldin et al.*, 2003] make interpretation of the discrepancy difficult.

[27] Halogen radicals in the model drive profound changes in the HO_x budget during O_3 depletion episodes. Without any halogens the production of HO_x is mainly due to the photolysis of CH_2O (~40%) with the photolysis of O_3 providing a smaller contribution (~20%). Most of the CH_2O (60%) in the model originates from surface emission (as opposed to production from methane and higher VOC oxidation) and thus acts as a primary HO_x source. The loss of HO_x is mainly (~75%) through the HO_2 self reaction to produce H_2O_2. With the inclusion of halogens this balance changes substantially. The primary source of HO_x becomes the reaction between Br and CH_2O. HOBr

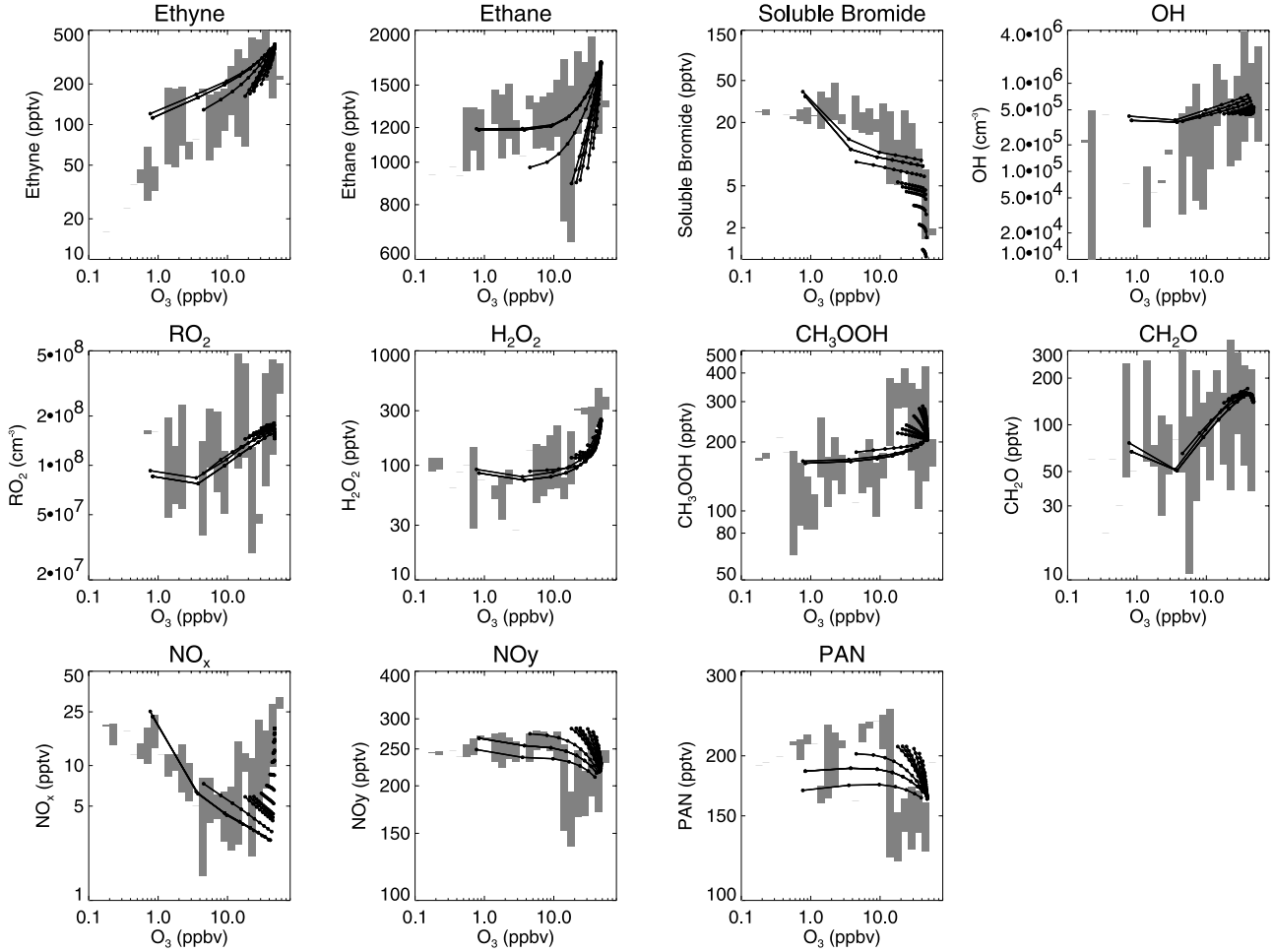

Figure 5. Chemical evolution during O_3 depletion events in the Arctic boundary layer in spring, plotted against the O_3 chemical coordinate. Aircraft measurements from TOPSE (north of 50°N, below 500 m altitude, March 23–May 22, 11:00–13:00 local time) are shown as grey bars (±1 standard deviation). Model results (section 3) are shown as lines for different initial bromide concentrations (0 to 43 pptv): the higher the initial bromide concentration, the larger the O_3 loss and thus the longer the line. The model simulations were conducted for 10 days starting at noon, and noontime concentrations are shown here (symbols on lines). See Table 1 for definitions of the lumped species.

acts as a temporary reservoir for HO_x, producing OH when photolysed and consuming HO_2 when produced. The uptake and subsequent destruction of HOBr in aerosols by R5 acts as a large HO_x sink. The rapid oxidation of hydrocarbons and carbonyls by Br or Cl increases the importance of organic peroxy radicals (CH_3O_2 and above) in the HO_x budget.

[28] We see from the above discussion that there is strong coupling and interchange between the HO_x and BrO_x families, with major sinks of HO_x serving as sources of BrO_x and vice versa, and with HOBr serving as a reservoir for both radical families. One can consider these families together with ClO_x (which plays little role and will not be discussed further) as components of a larger radical family $H/Cl/BrO_x$. The primary production of $H/Cl/BrO_x$ is from the photolysis of CH_2O and the primary sink is from peroxy–peroxy reactions. When $H/Cl/BrO_x$ is at steady state the photolysis of CH_2O is approximately balanced by the self reaction between RO_2 radicals. Reactions involving BrO_x play little role in producing or destroying $H/Cl/BrO_x$. Thus, the RO_2 concentration should be proportional to the square root of the CH_2O concentration regardless of the bromine chemistry. In both the model and the observations, CH_2O concentrations decline by a factor 4 as O_3 is depleted (Figure 5) and the RO_2 concentration responds by dropping by a factor of 2, in line with this simple analysis. The decline in CH_2O is driven by reaction with Br atoms. Thus the reaction between Br and CH_2O, rather than acting to increase HO_x concentrations, does in fact suppress them.

[29] Concentrations of H_2O_2 decrease during O_3 depletion events, while CH_3OOH initially increases and then decreases, both in the model and in the observations. The decline of H_2O_2 is due both to the decline of total peroxy radicals (RO_2) and to a shift in the partitioning of RO_2 to favor organic peroxy radicals, as discussed above. The latter shift favors CH_3OOH production, which is further favored by the drop in NO_x concentration at the onset of O_3 depletion events (the $CH_3O_2 + HO_2$ reaction proceeds faster under low NO_x concentration due to less competition from

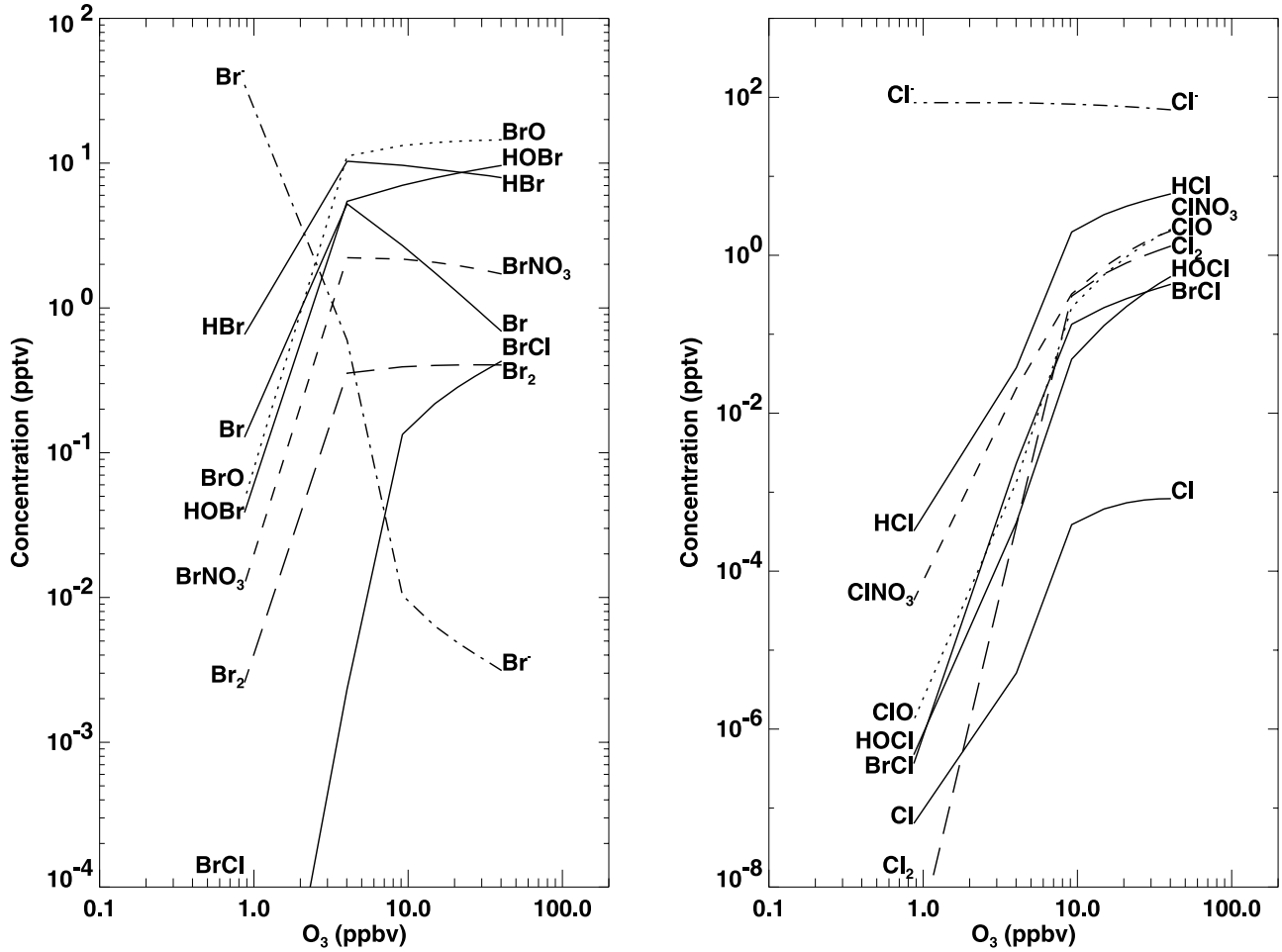

Figure 6. Modeled evolution of halogen concentrations for the simulation with 43 pptv of initial bromide, as a function of the O_3 concentration.

CH_3O_2 + NO). As O_3 concentrations drop below 10 ppbv, the recovery of NO_x as well as the decline in total RO_2 act to decrease CH_3OOH.

4.4. Nitrogen Oxide Radicals

[30] As O_3 concentrations decrease from 40 to 10 ppbv the measured NO_x exhibits a rapid decline from about 20 pptv to 3 pptv. As O_3 is further depleted the NO_x concentration recovers, eventually reaching similar concentrations to those observed in air masses with O_3 concentrations above 40 ppbv. The model reproduces this evolution as shown in Figure 5. In the model the decline and subsequent recovery in the NO_x concentration is due to a combination of $BrNO_3$ hydrolysis and NO_x emission from the snow. When BrO_x chemistry is active and O_3 concentrations are still high, formation and hydrolysis of $BrNO_3$ (ν = 0.3) leads to loss of NO_x. At lower O_3 concentrations, $BrNO_3$ formation is suppressed due to increases in both the NO/NO_2 and Br/BrO ratios.

[31] Both PAN and NO_y show a similar relationship with O_3, reflecting the dominant role of PAN in the composition of NO_y. The measurements show increases of PAN and NO_y during O_3 depletion events, and this is reproduced by the model (Figure 5). In the model, the rise in PAN is due to the oxidation of carbonyls and hydrocarbons by Cl and Br atoms, and is kept in check by the concurrent depletion of NO_x. The model study of *Shepson et al.* [1996] found much more rapid production of PAN during O_3 depletion events because they did not include $BrNO_3$ hydrolysis in their mechanism.

5. An Oscillatory System in Bromine-Catalyzed O_3 Depletion

[32] The search for oscillatory solutions in atmospheric chemistry models generates sporadic interest in the literature, both for theoretical curiosity and for possible implications for atmospheric stability [*Madronich and Hess*, 1994; *Poppe and Lustfeld*, 1996; *Tinsley and Field*, 2001]. We find in our photochemical simulation for the Arctic boundary layer described above that an oscillatory system with a period of 3 days develops under low O_3 conditions if the reactive uptake coefficients (γ) of HBr and HOBr are increased from 0.3 to 0.8 (alternatively this can be viewed as an increase in the aerosol surface area). Figure 7 shows the evolution of O_3, CH_2O, and NO_x and BrO concentrations under these conditions over a 30 day model simulation period with 43 pptv of initial bromide. The strong 3 day oscillation is evident. As bromine destroys O_3, the Br/BrO ratio increasingly favors HBr production over HOBr. This leads to an accumulation of

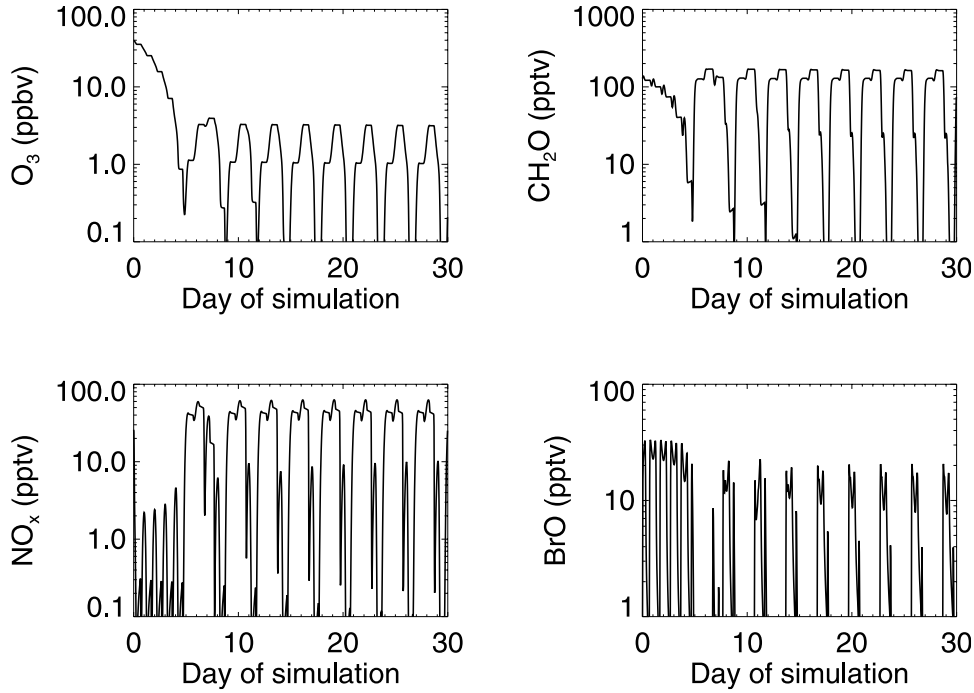

Figure 7. Temporal evolution of O_3, CH_2O, NO_x and BrO concentrations over a 30-day period for our standard simulation of O_3 depletion events in the Arctic boundary layer (c.f. Figure 4) but with enhanced aerosol uptake of HBr and HOBr (γ = 0.8, or equivalent increase in aerosol surface area). The initial bromide concentration is 43 pptv.

Br^- in the aerosol. Eventually virtually all of the model bromine resides in the aerosol (see Figure 6), suppressing BrO_x chemistry. Those species which are depleted by bromine radical chemistry, notably CH_2O and NO_x, increase in concentration, leading to O_3 production. The increase in O_3 concentration leads to increased HOBr concentration which in turn leads to an increased rate of recycling of bromine. This leads to net O_3 destruction and thus an oscillation. This appears to be the fastest oscillation calculated by a numerical model of the troposphere. Previous studies reviewed by *Tinsley and Field* [2001] have investigated cycles which act on timescales of a few weeks or more. Measurements in the Arctic boundary layer may offer the best opportunity of observing a chemical oscillation in the real atmosphere.

6. Conclusions

[33] Observations from the TOPSE aircraft campaign over the Arctic in March–May 2000 provide extensive chemical characterization of O_3 depletion events in the boundary layer. We used a combination of data analysis and photochemical modeling to investigate the processes controlling the coupled evolution of BrO_x-ClO_x-HO_x-NO_x radicals and their reservoirs.

[34] Ethane and ethyne observations during TOPSE indicate that Cl radical chemistry is important only during the early stages of O_3 depletion while Br radical chemistry remains active even as O_3 drops below 1 ppbv. We reproduce these results in our model. As the O_3 concentration decreases below 5 ppb, accumulation of Br^- in the aerosol leads Br_2 production to compete with BrCl production as a sink of HOBr leading to a reduction in the rate of Cl radical production. Also, the reaction between aerosol phase BrCl and Br^- to produce Br_2Cl^- further inhibits the release of BrCl. These two processes lead to a marked reduction in Cl chemistry below 10 ppbv of O_3.

[35] Measured total peroxy radical concentrations (RO_2) drop by a factor of 2 during O_3 depletion events, a trend well reproduced by our model. During these events there are strong interchanges between HO_x and BrO_x radicals, and HOBr serves as a major reservoir for both. We define a generalized H/Cl/BrO_x radical family to account for this coupling. Production of this family is mostly from the photolysis of CH_2O emitted from the snow, and loss is mostly by the self reactions of peroxy radicals. Thus, at steady state the RO_2 concentration is proportional to the square root of the CH_2O concentration. Measured and simulated CH_2O concentrations drop by a factor of 4 during O_3 depletion events due to reaction with Br atoms, explaining the observed decrease in RO_2 concentrations.

[36] Observed NO_x concentrations show a marked decline during the early stages of O_3 depletion with subsequent recovery as the O_3 concentration drops below 10 ppbv. We reproduce this feature and ascribe the initial NO_x depletion to $BrNO_3$ hydrolysis. As the O_3 concentration continues to drop, both the Br/BrO and NO/NO_2 ratios increase which leads to a reduction in the $BrNO_3$ concentration and thus the magnitude of the NO_x sink. The emission of NO_x from the snow then leads to a recovery in the NO_x concentration. The magnitude of this recovery is obviously dependent upon the strength of the surface source and thus may vary geographically and seasonally.

[37] Outside of O_3 depletion episodes, our model calculations suggest that aerosol phase reactions of HNO_4 with

HNO_2 and I^- could represent a substantial sink for NO_x. There is an obvious need for HNO_4 measurements in the Arctic boundary layer and for better characterization of HNO_4 chemistry.

[38] Our photochemical model simulation for the Arctic boundary layer shows a large-amplitude oscillation for O_3 with a period of 3 days under certain realistic conditions with high bromine. The period of the oscillation is much shorter than previously reported oscillations in tropospheric chemistry mechanisms. Although it could be nothing more than a theoretical curiosity, since external forcing (such as from transport) is likely to disrupt it, it may because of it short period afford an opportunity for observing an oscillation in the real atmosphere.

[39] **Acknowledgments.** This work was funded by the Atmospheric Chemistry Program of the U.S. National Science Foundation.

References

Abbatt, J. P. D., and M. J. Molina, The heterogeneous reaction of HOCl + HCl → Cl_2 + H_2O on ice and nitric-acid trihydrate: Reaction probabilities and stratospheric implications, *Geophys. Res. Lett.*, *19*, 461–464, 1992.

Allanic, A., R. Oppliger, and M. J. Rossi, Real-time kinetics of the uptake of HOBr and $BrONO_2$ on ice and in the presence of HCl in the temperature range 190–200K, *J. Geophys. Res.*, *102*, 23,529–23,541, 1997.

Amels, P., H. Elias, U. Gotz, U. Steinges, and K. J. Wannowius, Kinetic investigation of the stability of peroxynitric acid and of its reaction with sulfur(IV) in aqueous solution, in *Heterogeneous and Liquid Phase Processes*, *Transport and Chemical Transformation of Pollutants in the Troposphere*, vol. 2, edited by P. Warneck, pp. 77–88, Springer-Verlag, New York, 1996.

Atlas, E., B. Ridley, and C. Cantrell, The Tropospheric Ozone Production about the Spring Equinox (TOPSE) experiment: Introduction, *J. Geophys. Res.*, doi:10.1029/2002JD003172, in press, 2003.

Baker, A. R., C. Tunnicliffe, and T. D. Jickells, Iodine speciation and deposition fluxes from the marine atmosphere, *J. Geophys. Res.*, *106*, 28,743–28,749, 2001.

Barrie, L. A., and R. M. Hoff, The oxidation rate and residence time of sulfur-dioxide in the Arctic atmosphere, *Atmos. Environ.*, *18*, 2711–2722, 1984.

Barrie, L. A., J. W. Bottenheim, R. C. Schnell, P. J. Crutzen, and R. A. Rasmussen, Ozone destruction and photochemical-reactions at polar sunrise in the lower Arctic atmosphere, *Nature*, *334*, 138–141, 1988.

Bartlett, W. P., and D. W. Margerum, Temperature dependencies of the Henry's Law constant and the aqueous phase dissociation constant of bromine chloride, *Environ. Sci. Technol.*, *33*, 3410–3414, 1999.

Beckwith, R. C., T. X. Wang, and D. W. Margerum, Equilibrium and kinetics of bromine hydrolysis, *Inorg. Chem.*, *35*, 995–1000, 1996.

Beine, H. J., D. A. Jaffe, F. Stordal, M. Engardt, S. Solberg, N. Schmidbauer, and K. Holmen, NO_x during ozone depletion events in the arctic troposphere at Ny-Alesund, Svalbard, *Tellus Ser. B*, *49*, 556–565, 1997.

Blake, N. J., D. R. Blake, B. C. Sive, A. S. Katzenstein, S. Meinardi, O. W. Wingenter, E. L. Atlas, F. Flocke, B. A. Ridley, and F. S. Rowland, The seasonal evolution of NMHCs and light alkyl nitrates at mid to high northern latitudes during TOPSE, *J. Geophys. Res.*, *108*(D4), 8359, doi:10.1029/2001JD001467, 2003.

DeMore, W. B., chemical kinetic and photochemical data for use in stratospheric modeling, Evalution number 12, *JPL Publ. Tech Rep 97-4*, NASA Jet Prop. Lab., Pasadena, Calif., 1997.

Dentener, F., J. Williams, and S. Metzger, Aqueous phase reaction of HNO_4: The impact on tropospheric chemistry, *J. Atmos. Chem.*, *41*, 109–134, 2002.

Fan, S.-M., and D. J. Jacob, Surface ozone depletion in Arctic spring sustained by bromine reactions on aerosols, *Nature*, *359*, 522–524, 1992.

Fried, A., et al., Tunable diode laser measurements of formaldehyde during the TOPSE 2000: Distributions, trends, and model Comparisons, *J. Geophys. Res.*, *108*(D4), 8365, doi:10.1029/2002JD002208, 2003.

Haag, W. R., and J. Hoigné, Ozonation of bromide-containing waters: Kinetics of formation of hypobromous acid and bromate, *Environ. Sci. Technol.*, *17*, 261–267, 1983.

Hanson, D. R., A. R. Ravishankara, and E. R. Lovejoy, Reaction of $BrONO_2$ with H_2O on submicron sulfuric acid aerosol and the implications for the lower stratosphere, *J. Geophys. Res.*, *101*, 9063–9069, 1996.

Hausmann, M., and U. Platt, Spectroscopic measurement of bromine oxide and ozone in the high arctic during Polar Sunrise Experiment 1992, *J. Geophys. Res.*, *99*, 25,399–25,413, 1994.

Honrath, R. E., S. Guo, M. C. Peterson, M. P. Dziobak, J. E. Dibb, and M. A. Arsenault, Photochemical production of gas phase NO_x from ice crystal NO_3^-, *J. Geophys. Res.*, *105*, 24,183–24,190, 2000.

Honrath, R. E., Y. Lu, M. C. Peterson, J. E. Dibb, M. A. Arsenault, N. J. Cullen, and K. Steffen, Vertical fluxes of NO_x, HONO and HNO_3 above the snowpack at Summit, Greenland, *Atmos. Environ.*, *36*, 2629–2640, 2002.

Huthwelker, T., T. Peter, B. P. Luo, S. L. Clegg, K. S. Carslaw, and P. Brimblecombe, Solubility of HOCl in water and aqueous H_2SO_4 to stratospheric temperatures, *J. Atmos. Chem.*, *21*, 81–95, 1995.

Hutterli, M. A., R. C. Röthlisbereger, and R. C. Bales, Atmosphere-to-snow-to-firn transfer studies of HCHO at Summit, Greenland, *Geophys. Res. Lett.*, *26*, 1691–1694, 1999.

Hutterli, M. A., J. R. McConnell, R. W. Stewart, H.-W. Jacobi, and R. C. Bales, Impact of temperature-driven cycling of hydrogen peroxide (H_2O_2) between air and snow on the planetary boundary layer, *J. Geophys. Res.*, *106*, 15,395–15,404, 2001.

Jacob, D. J., Heterogeneous chemistry and tropospheric ozone, *Atmos. Environ.*, *34*, 2131–2159, 2000.

Jaeglé, L., et al., Photochemistry of HO_x in the upper troposphere at northern midlatitudes, *J. Geophys. Res.*, *105*, 3877–3892, 2000.

Jobson, B. T., H. Niki, Y. Yokouchi, J. Bottenheim, F. Hopper, and R. Leaitch, Measurements of C_2-C_6 hydrocarbons during the Polar Sunrise 1992 Experiment: Evidence for Cl atom and Br atom chemistry, *J. Geophys. Res.*, *99*, 25,355–25,368, 1994.

Jones, A. E., R. Weller, P. S. Anderson, H.-W. Jacobi, E. W. Wolff, O. Schrems, and H. Miller, Measurements of NO_x emissions from the Antarctic snowpack, *Geophys. Res. Lett.*, *28*, 1499–1502, 2001.

Kelley, C. M., and H. V. Tartar, On the system: bromine-water, *J. Am. Chem. Soc.*, *78*, 5752–5756, 1956.

Kosak-Channing, L. F., and G. R. Helz, Solubility of ozone in aqueous solutions of 0–0.6M ionic strength at 5°–30°C, *Environ. Sci. Technol.*, *17*, 145–149, 1983.

Kumar, K., and D. W. Margerum, Kinetics and mechanism of general-acid-assisted oxidation of bromide by hypochlorite and hypochlorous acid, *Inorg. Chem.*, *26*, 2706–2711, 1987.

Leriche, M., D. Voisin, N. Chaumerliac, A. Monod, and B. Aumont, A model for tropospheric multiphase chemistry: Application to one cloudy event during the CIME experiment, *Atmos. Environ.*, *34*, 5015–5036, 2000.

Li, S.-M., Equilibrium of particle nitrite with gas-phase HONO: Tropospheric measurements in the high arctic during polar sunrise, *J. Geophys. Res.*, *99*, 25,469–25,478, 1994.

Li, Z. J., R. R. Friedl, S. B. Moore, and S. P. Sander, Interaction of peroxynitric acid with solid H_2O ice, *J. Geophys. Res.*, *101*, 6795–6802, 1996.

Logager, T., and K. Sehested, Formation and decay of peroxynitric acid – A pulse radiolysis study, *J. Phys. Chem.*, *97*, 10,047–10,052, 1993.

Madronich, S., and P. Hess, The oxidizing capacity of the troposphere and its changes, in *Physic-Chemical Behavior of Atmospheric Pollutants Proceedings of the Sixth European Symposium*, *Held in Varese (Italy) 18–22 October 1993*, edited by G. Angeletti and G. Restelli, pp. 5–13, Eur. Commission, Luxembourg, 1994.

Magi, L., F. Schweitzer, C. Pallares, S. Cherif, P. Mirabel, and C. George, Investigation of the uptake rate of ozone and methyl hydroperoxide by water surfaces, *J. Phys. Chem. A*, *101*, 4943–4949, 1997.

Martinez, M., T. Arnold, and D. Perner, The role of bromine and chlorine chemistry for arctic ozone depletion events in Ny-Alesund and comparison with model calculations, *Ann. Geophys. Atmos. Hydro. Space Sci.*, *17*, 941–956, 1999.

Mauldin, R. L., C. A. Cantrell, M. A. Zondlo, E. Kosciuch, B. A. Ridley, R. Weber, and F. E. Eisele, Measurements of OH, H_2SO_4, and MSA during TOPSE, *J. Geophys. Res*, doi:10.1029/2002JD002295, in press, 2003.

Michalowski, B. A., J. S. Francisco, S.-M. Li, L. A. Barrie, J. W. Bottenheim, and P. B. Shepson, A computer model study of multiphase chemistry in the Arctic boundary layer during polar sunrise, *J. Geophys. Res.*, *105*, 15,131–15,145, 2000.

Monks, P. S., A review of the observations and origins of the spring ozone maximum, *Atmos. Environ.*, *34*, 3545–3561, 2000.

Oltmans, S. J., Surface ozone measurements in clean air, *J. Geophys. Res.*, *86*, 1174–1180, 1981.

Oltmans, S. J., and W. D. Komhyr, Surface ozone distributions and variations from 1973–1984 measurements at the NOAA Geophysical Monitoring for Climatic Change Baseline observatories, *J. Geophys. Res.*, *91*, 5229–5236, 1986.

Orlando, J. J., B. Ramacher, and G. S. Tyndall, Upper limits for the rate coefficients for reactions of BrO with formaldehyde and HBr, *Geophys. Res. Letts.*, *27*, 2633–2636, 2000.

Poppe, D., and H. Lustfeld, Nonlinearities in the gas phase chemistry of the troposphere: Oscillating concentration in a simplified mechanism, *J. Geophys. Res.*, *101*, 14,373–14,380, 1996.

Ramacher, B., J. Rudolph, and R. Koppmann, Hydrocarbon measurements during tropospheric ozone depletion events: Evidence for halogen atom chemistry, *J. Geophys. Res.*, *104*, 3633–3653, 1999.

Ramacher, B., J. J. Orlando, and G. S. Tyndall, Temperature-dependent rate coefficient measurements for the reaction of bromine atoms with a series of aldehydes, *Int. J. Chem. Kinet.*, *32*, 460–465, 2000.

Ramacher, B., J. J. Orlando, and G. S. Tyndall, Temperature-dependent rate coefficient measurements for the reaction of bromine atoms with trichloroethene, ethene, acetylene, and tetrachloroethene in air, *Int. J. Chem. Kinet.*, *33*, 198–211, 2001.

Régimbal, J.-M., and M. Mozurkewich, Peroxynitric acid decay mechanisms and kinetics at low pH, *J. Phys. Chem. A*, *101*, 8822–8829, 1997.

Ridley, B., et al., Is the Arctic surface layer a source and sink of NO_x in winter/spring?, *J. Atmos. Chem.*, *36*, 1–22, 2000.

Ridley, B. A., et al., Ozone depletion events observed in the high latitude surface layer during the TOPSE aircraft program, *J. Geophys. Res.*, *108*(D4), 8356, doi:10.1029/2001JD001507, 2003.

Robinson, G. N., D. R. Worsnop, J. T. Jayne, C. E. Kolb, and P. Davidovits, Heterogeneous uptake of $ClONO_2$ and N_2O_5 by sulfuric acid solutions, *J. Geophys. Res.*, *102*, 3583–3601, 1997.

Rudolph, J., B. R. Fu, A. Thompson, K. Anlauf, and J. Bottenheim, Halogen atom concentrations in the Arctic troposphere derived from hydrocarbon measurements: Impact on the budget of formaldehyde, *Geophys. Res. Lett.*, *26*, 2941–2944, 1999.

Sander, R., and P. J. Crutzen, Model study indicating halogen activation and ozone destruction in polluted air masses transported to the sea, *J. Geophys. Res.*, *101*, 9121–9138, 1996.

Sander, R., R. Vogt, G. W. Harris, and P. J. Crutzen, Modeling the chemistry of ozone, halogen compounds and hydrocarbons in the arctic troposphere during spring, *Tellus Ser. B*, *49*, 522–532, 1997.

Sander, S. P., et al., Chemical kinetics and photochemical data for use in stratospheric modeling, Evalution number 13, *JPL Publ. Tech Rep 00-3*, NASA, Jet Prop. Lab., Pasadena, Calif., 2000.

Scheuer, E., R. W. Talbot, J. E. Dibb, G. K. Seid, L. DeBell, and B. Lefer, Seasonal distributions of fine aerosol sulfate in the North American Arctic Basin during TOPSE, *J. Geophys. Res.*, doi:10.1029/2001JD001364, in press, 2003.

Schweitzer, F., P. Mirabel, and C. George, Uptake of hydrogen halides by water droplets, *J. Phys. Chem. A*, *104*, 72–76, 2000.

Shepson, P. B., A.-P. Sirju, J. F. Hopper, L. A. Barrie, V. Young, H. Niki, and H. Dryfhout, Sources and sinks of carbonyl compounds in the Arctic Ocean boundary layer: Polar Ice Floe Experiment, *J. Geophys. Res.*, *101*, 21,081–21,089, 1996.

Shetter, R. E., and M. Muller, Photolysis frequency measurements using actinic flux spectroradiometry during the PEM-Tropics mission: Instrumentation description and some results, *J. Geophys. Res.*, *104*, 5647–5661, 1999.

Sirois, A., and L. A. Barrie, Arctic lower tropospheric aerosol trends and composition at Alert, Canada: 1980–1995, *J. Geophys. Res.*, *104*, 11,599–11,618, 1999.

Snow, J. A., B. G. Heikes, J. T. Merrill, A. J. Wimmers, J. L. Moody, and C. A. Cantrell, Winter-spring evolution and variability of HO_x reservoir species, hydrogen peroxide and methyl hydroperoxide, in the northern mid to high-latitudes, *J. Geophys. Res.*, doi:10.1029/2002JD002172, in press, 2003.

Sumner, A. L., and P. B. Shepson, Snowpack production of formaldehyde and its effect on the Arctic troposphere, *Nature*, *398*, 230–233, 1999.

Tinsley, M. R., and R. J. Field, Steady state instability and oscillation in simplified models of tropospheric chemistry, *J. Phys. Chem. A.*, *105*, 11,212–11,219, 2001.

Wang, T. X., and D. W. Margerum, Kinetics of reversible chlorine hydrolysis: Temperature-dependence and general acid/base assisted mechanisms, *Inorg. Chem.*, *33*, 1050–1055, 1994.

Wang, T. X., M. D. Kelley, J. N. Cooper, R. C. Beckwith, and D. W. Margerum, Equilibrium, kinetic and UV-spectral characteristics of aqueous bromine chloride, bromine and chlorine species, *Inorg. Chem.*, *33*, 5872–5878, 1994.

Warneck, P., The relative importance of various pathways for the oxidation of sulfur dioxide and nitrogen dioxide in sunlit continental fair weather clouds, *Phys. Chem. Chem. Phys.*, *1*, 5471–5483, 1999.

Waschewsky, G. C. G., and J. P. D. Abbatt, HOBr in sulfuric acid solutions: Solubility and reaction with HCl as a function of temperature and concentration, *J. Phys. Chem. A*, *103*, 5312–5320, 1999.

Wessel, S., S. Aoki, P. Winkler, R. Weller, A. Herber, H. Gernandt, and O. Schrems, Tropospheric ozone depletion in polar regions – A comparison of observations in the Arctic and Antarctic, *Tellus Ser. B*, *50*, 34–50, 1998.

Wilhelm, E., R. Battino, and R. J. Wilcock, Low-pressure solubility of gases in liquid water, *Chem. Rev.*, *77*, 219–262, 1977.

Wolff, E. W., Nitrate in polar snow, in *Ice Core Studies of Biogeochemical Cycles*, *NATO ASI Ser. I*, edited by Robert J. Delmas, pp. 195–224, Springer-Verlag, New York, 1995.

Yokouchi, Y., H. Akimoto, L. A. Barrie, J. W. Bottenheim, K. Anlauf, and B. T. Jobson, Serial gas-chromatographic mass-spectrometric measurements of some volatile organic-compounds in the Arctic atmosphere during the 1992 Polar Sunrise Experiment, *J. Geophys. Res.*, *99*, 25,379–25,389, 1994.

E. Atlas, C. A. Cantrell, F. Eisele, F. Flocke, A. Fried, R. L. Mauldin, B. A. Ridley, J. Walega, A. J. Weinheimer, and B. Wert, Atmospheric Chemistry Division, National Center for Atmospheric Research, Boulder, CO 80305, USA.

D. Blake, Department of Chemistry, University of California, Irvine, Irvine, CA 92697, USA.

J. Dibb and R. Talbot, Climate Change Research Center, University of New Hampshire, Durham, NH 03824, USA.

M. J. Evans and D. J. Jacob, Division of Engineering and Applied Science, Harvard University, Cambridge, MA 02138, USA. (mje@ilo.harvard.edu)

B. Heikes, School of Oceanography, University of Rhode Island, Narragansett, RI 02882, USA.

J. Snow, University of Washington Bothell, Bothell, WA 98011, USA.